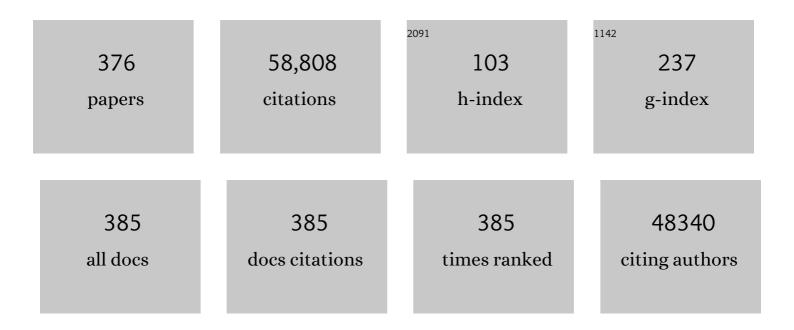
## Nathan S Lewis

List of Publications by Year in descending order

Source: https://exaly.com/author-pdf/117288/publications.pdf Version: 2024-02-01



#	Article	IF	CITATIONS
1	Catalytic open-circuit passivation by thin metal oxide films of p-Si anodes in aqueous alkaline electrolytes. Energy and Environmental Science, 2022, 15, 334-345.	15.6	8
2	Experimental and Theoretical Comparison of Potential-dependent Methylation on Chemically Exfoliated WS <sub>2</sub> and MoS <sub>2</sub> . ACS Applied Materials & Interfaces, 2022, 14, 9744-9753.	4.0	2
3	Strain-Based Chemiresistive Polymer-Coated Graphene Vapor Sensors. ACS Omega, 2022, 7, 10765-10774.	1.6	2
4	Plastic Morphological Response to Spectral Shifts during Inorganic Phototropic Growth. Jacs Au, 2022, 2, 865-874.	3.6	3
5	The role of concentrated solar power with thermal energy storage in least-cost highly reliable electricity systems fully powered by variable renewable energy. Advances in Applied Energy, 2022, 6, 100091.	6.6	56
6	Failure Modes of Platinized pn <sup>+</sup> -GaInP Photocathodes for Solar-Driven H <sub>2</sub> Evolution. ACS Applied Materials & Interfaces, 2022, 14, 26622-26630.	4.0	4
7	Demonstration of a Sensitive and Stable Chemical Gas Sensor Based on Covalently Functionalized MoS <sub>2</sub> . , 2022, 4, 1475-1480.		8
8	Optical and electrochemical effects of H <sub>2</sub> and O <sub>2</sub> bubbles at upward-facing Si photoelectrodes. Energy and Environmental Science, 2021, 14, 414-423.	15.6	26
9	Defect-Tolerant TiO <sub>2</sub> -Coated and Discretized Photoanodes for >600 h of Stable Photoelectrochemical Water Oxidation. ACS Energy Letters, 2021, 6, 193-200.	8.8	25
10	Primary Corrosion Processes for Polymer-Embedded Free-Standing or Substrate-Supported Silicon Microwire Arrays in Aqueous Alkaline Electrolytes. Nano Letters, 2021, 21, 1056-1061.	4.5	3
11	Design of robust 2,2′-bipyridine ligand linkers for the stable immobilization of molecular catalysts on silicon(111) surfaces. Physical Chemistry Chemical Physics, 2021, 23, 9921-9929.	1.3	6
12	Decoupled electrochemical water-splitting systems: a review and perspective. Energy and Environmental Science, 2021, 14, 4740-4759.	15.6	172
13	X-ray Photoelectron Spectroscopy and Resonant X-ray Spectroscopy Investigations of Interactions between Thin Metal Catalyst Films and Amorphous Titanium Dioxide Photoelectrode Protection Layers. Chemistry of Materials, 2021, 33, 1265-1275.	3.2	15
14	Assessing Effects of Near-Field Synergistic Light Absorption on Ordered Inorganic Phototropic Growth. Journal of the American Chemical Society, 2021, 143, 3693-3696.	6.6	5
15	Preseeded Optical Scatterers as a Template for Enhancing Order in Inorganic Phototropic Growth. Journal of Physical Chemistry C, 2021, 125, 9571-9581.	1.5	1
16	Wind and Solar Resource Droughts in California Highlight the Benefits of Long-Term Storage and Integration with the Western Interconnect. Environmental Science & Technology, 2021, 55, 6214-6226.	4.6	39
17	Origin of the Electrical Barrier in Electrolessly Deposited Platinum Nanoparticles on p-Si Surfaces. Journal of Physical Chemistry C, 2021, 125, 17660-17670.	1.5	6
18	Opportunities for flexible electricity loads such as hydrogen production from curtailed generation. Advances in Applied Energy, 2021, 3, 100051.	6.6	41

#	Article	IF	CITATIONS
19	GaAs Microisland Anodes Protected by Amorphous TiO <sub>2</sub> Films Mitigate Corrosion Spreading During Water Oxidation in Alkaline Electrolytes. ACS Energy Letters, 2021, 6, 3709-3714.	8.8	7
20	Investigations of the stability of etched or platinized p-InP(100) photocathodes for solar-driven hydrogen evolution in acidic or alkaline aqueous electrolytes. Energy and Environmental Science, 2021, 14, 6007-6020.	15.6	33
21	Investigations of the stability of GaAs for photoelectrochemical H <sub>2</sub> evolution in acidic or alkaline aqueous electrolytes. Journal of Materials Chemistry A, 2021, 9, 22958-22972.	5.2	9
22	Nanotechnology for catalysis and solar energy conversion. Nanotechnology, 2021, 32, 042003.	1.3	44
23	Geophysical constraints on the reliability of solar and wind power worldwide. Nature Communications, 2021, 12, 6146.	5.8	90
24	Optical and Electrochemical Effects of Gas Bubbles Generating Passive Convection in Solar Fuels Devices. ECS Meeting Abstracts, 2021, MA2021-02, 1310-1310.	0.0	0
25	Long-duration energy storage for reliable renewable electricity: The realistic possibilities. Bulletin of the Atomic Scientists, 2021, 77, 281-284.	0.2	1
26	Understanding the Stability of Etched or Platinized p-GaInP Photocathodes for Solar-Driven H <sub>2</sub> Evolution. ACS Applied Materials & Interfaces, 2021, 13, 57350-57361.	4.0	6
27	Reductant-Activated, High-Coverage, Covalent Functionalization of 1T′-MoS <sub>2</sub> . , 2020, 2, 133-139.		21
28	High Broadband Light Transmission for Solar Fuels Production Using Dielectric Optical Waveguides in TiO <sub>2</sub> Nanocone Arrays. Nano Letters, 2020, 20, 502-508.	4.5	14
29	Spontaneous Formation of >90% Optically Transmissive, Electrochemically Active CoP Films for Photoelectrochemical Hydrogen Evolution. Journal of Physical Chemistry Letters, 2020, 11, 14-20.	2.1	8
30	Enhanced stability of silicon for photoelectrochemical water oxidation through self-healing enabled by an alkaline protective electrolyte. Energy and Environmental Science, 2020, 13, 4132-4141.	15.6	14
31	Would firm generators facilitate or deter variable renewable energy in a carbon-free electricity system?. Applied Energy, 2020, 279, 115789.	5.1	12
32	Failure modes of protection layers produced by atomic layer deposition of amorphous TiO <sub>2</sub> on GaAs anodes. Energy and Environmental Science, 2020, 13, 4269-4279.	15.6	15
33	Evaluation of sputtered nickel oxide, cobalt oxide and nickel–cobalt oxide on n-type silicon photoanodes for solar-driven O2(g) evolution from water. Journal of Materials Chemistry A, 2020, 8, 13955-13963.	5.2	9
34	Atomic force microscopy: Emerging illuminated and <i>operando</i> techniques for solar fuel research. Journal of Chemical Physics, 2020, 153, 020902.	1.2	25
35	Path-Dependent Morphological Evolution of Se–Te Mesostructures Prepared by Inorganic Phototropic Growth. Journal of the American Chemical Society, 2020, 142, 19840-19843.	6.6	3
36	Effects of Deep Reductions in Energy Storage Costs on Highly Reliable Wind and Solar Electricity Systems. IScience, 2020, 23, 101484.	1.9	36

#	Article	IF	CITATIONS
37	Role of Long-Duration Energy Storage in Variable Renewable Electricity Systems. Joule, 2020, 4, 1907-1928.	11.7	238
38	Cathodic NH <sub>4</sub> <sup>+</sup> leaching of nitrogen impurities in CoMo thin-film electrodes in aqueous acidic solutions. Sustainable Energy and Fuels, 2020, 4, 5080-5087.	2.5	14
39	Optically tunable mesoscale CdSe morphologies <i>via</i> inorganic phototropic growth. Journal of Materials Chemistry C, 2020, 8, 12412-12417.	2.7	8
40	Genesis and Propagation of Fractal Structures During Photoelectrochemical Etching of n-Silicon. ACS Applied Materials & Interfaces, 2020, 12, 17018-17028.	4.0	4
41	Defect-Seeded Atomic Layer Deposition of Metal Oxides on the Basal Plane of 2D Layered Materials. Nano Letters, 2020, 20, 2632-2638.	4.5	7
42	Surface Passivation and Positive Band-Edge Shift of p-Si(111) Surfaces Functionalized with Mixed Methyl/Trifluoromethylphenylacetylene Overlayers. Journal of Physical Chemistry C, 2020, 124, 16338-16349.	1.5	1
43	Si Microwire-Array Photocathodes Decorated with Cu Allow CO <sub>2</sub> Reduction with Minimal Parasitic Absorption of Sunlight. ACS Energy Letters, 2020, 5, 2528-2534.	8.8	33
44	Macroscale and Nanoscale Photoelectrochemical Behavior of p-Type Si(111) Covered by a Single Layer of Graphene or Hexagonal Boron Nitride. ACS Applied Materials & Interfaces, 2020, 12, 11551-11561.	4.0	10
45	Conformal SnO <sub>x</sub> heterojunction coatings for stabilized photoelectrochemical water oxidation using arrays of silicon microcones. Journal of Materials Chemistry A, 2020, 8, 9292-9301.	5.2	12
46	Effects of bubbles on the electrochemical behavior of hydrogen-evolving Si microwire arrays oriented against gravity. Energy and Environmental Science, 2020, 13, 1808-1817.	15.6	37
47	Isotopically Selective Quantification by UPLC-MS of Aqueous Ammonia at Submicromolar Concentrations Using Dansyl Chloride Derivatization. ACS Energy Letters, 2020, 5, 1532-1536.	8.8	34
48	Increased spatial randomness and disorder of nucleates in dark-phase electrodeposition lead to increased spatial order and pattern fidelity in phototropically grown Se–Te electrodeposits. Nanoscale, 2020, 12, 22478-22486.	2.8	2
49	Passivation of Defects in Macroscopic Graphene Sheets Via Selective Atomic Layer Deposition of Metal Oxides. ECS Meeting Abstracts, 2020, MA2020-01, 834-834.	0.0	0
50	Nucleation, Pattern Development, and Fidelity in the Photoelectrodeposition of Se-Te Nanostructures. ECS Meeting Abstracts, 2020, MA2020-01, 1216-1216.	0.0	0
51	Revealing the Surface Corrosion Chemistry and Kinetic Stabilization at Photoelectrochemical Interfaces for Solar-Driven Water-Splitting. ECS Meeting Abstracts, 2020, MA2020-01, 1773-1773.	0.0	0
52	Phototropic Growth of Semiconductor Mesostructures Exhibits Auto-Optimizing Interfacial Light Absorption. ECS Meeting Abstracts, 2020, MA2020-01, 1191-1191.	0.0	0
53	Enhanced Stability and Efficiency for Photoelectrochemical Iodide Oxidation by Methyl Termination and Electrochemical Pt Deposition on n-Type Si Microwire Arrays. ACS Energy Letters, 2019, 4, 2308-2314.	8.8	4
54	Inorganic Phototropism in Electrodeposition of Se–Te. Journal of the American Chemical Society, 2019, 141, 18658-18661.	6.6	8

#	Article	IF	CITATIONS
55	Vibrational Sum Frequency Generation Spectroscopy Measurement of the Rotational Barrier of Methyl Groups on Methyl-Terminated Silicon(111) Surfaces. Journal of Physical Chemistry Letters, 2019, 10, 5434-5439.	2.1	4
56	Enhancing the activity of oxygen-evolution and chlorine-evolution electrocatalysts by atomic layer deposition of TiO <sub>2</sub> . Energy and Environmental Science, 2019, 12, 358-365.	15.6	78
57	A prospective on energy and environmental science. Energy and Environmental Science, 2019, 12, 16-18.	15.6	14
58	Influence of Substrates on the Long-Range Order of Photoelectrodeposited Se–Te Nanostructures. Nano Letters, 2019, 19, 1295-1300.	4.5	3
59	Characterization of Electronic Transport through Amorphous TiO <sub>2</sub> Produced by Atomic Layer Deposition. Journal of Physical Chemistry C, 2019, 123, 20116-20129.	1.5	68
60	Integration of electrocatalysts with silicon microcone arrays for minimization of optical and overpotential losses during sunlight-driven hydrogen evolution. Sustainable Energy and Fuels, 2019, 3, 2227-2236.	2.5	7
61	Femtosecond time-resolved two-photon photoemission studies of ultrafast carrier relaxation in Cu2O photoelectrodes. Nature Communications, 2019, 10, 2106.	5.8	29
62	Decoupling H <sub>2</sub> (g) and O <sub>2</sub> (g) Production in Water Splitting by a Solar-Driven V <sup>3+/2+</sup> (aq,H <sub>2</sub> SO <sub>4</sub> ) KOH(aq) Cell. ACS Energy Letters, 2019, 4, 968-976.	8.8	33
63	Crystalline nickel, cobalt, and manganese antimonates as electrocatalysts for the chlorine evolution reaction. Energy and Environmental Science, 2019, 12, 1241-1248.	15.6	78
64	Vapor-fed electrolysis of water using earth-abundant catalysts in Nafion or in bipolar Nafion/poly(benzimidazolium) membranes. Sustainable Energy and Fuels, 2019, 3, 3611-3626.	2.5	14
65	Emergent Growth of Semiconductor Nanopatterns Via Directed Illumination. ECS Meeting Abstracts, 2019, , .	0.0	0
66	Physical Translation of Optical Excitation into Nanoscale Semiconductor Morphologies. ECS Meeting Abstracts, 2019, , .	0.0	0
67	Inorganic Phototropic Growth of Nanoscale Semiconductor Deposits. ECS Meeting Abstracts, 2019, , .	0.0	0
68	Morphological Evolution of Photoelectrodeposited Semiconductor Nanopatterns in Response to Dynamic Optical Inputs. ECS Meeting Abstracts, 2019, , .	0.0	0
69	Evaluating the Intrinsic Material Stability at the Semiconductor/Electrolyte Interface for Solar Fuel Production. ECS Meeting Abstracts, 2019, , .	0.0	0
70	(Invited) Materials By Design Principles in Artificial Photosynthesis: Discovery and Synergistic Integration of Light Absorbers, Electrocatalysts and Membranes for Complete, Stable, Efficient, and Safe Solar Fuels Generator. ECS Meeting Abstracts, 2019, , .	0.0	0
71	Semiconductor Nanostructure Tailoring Via Spontaneous Interface Shaping for Light-Collection Maximization. ECS Meeting Abstracts, 2019, , .	0.0	0
72	Geophysical constraints on the reliability of solar and wind power in the United States. Energy and Environmental Science, 2018, 11, 914-925.	15.6	211

#	Article	IF	CITATIONS
73	Performance and failure modes of Si anodes patterned with thin-film Ni catalyst islands for water oxidation. Sustainable Energy and Fuels, 2018, 2, 983-998.	2.5	24
74	Relative costs of transporting electrical and chemical energy. Energy and Environmental Science, 2018, 11, 469-475.	15.6	46
75	Hydrogen Evolution with Minimal Parasitic Light Absorption by Dense Co–P Catalyst Films on Structured p-Si Photocathodes. ACS Energy Letters, 2018, 3, 612-617.	8.8	41
76	In situ recombination junction between p-Si and TiO <sub>2</sub> enables high-efficiency monolithic perovskite/Si tandem cells. Science Advances, 2018, 4, eaau9711.	4.7	122
77	The Predominance of Hydrogen Evolution on Transition Metal Sulfides and Phosphides under CO <sub>2</sub> Reduction Conditions: An Experimental and Theoretical Study. ACS Energy Letters, 2018, 3, 1450-1457.	8.8	66
78	Net-zero emissions energy systems. Science, 2018, 360, .	6.0	1,165
79	Tin Oxide as a Protective Heterojunction with Silicon for Efficient Photoelectrochemical Water Oxidation in Strongly Acidic or Alkaline Electrolytes. Advanced Energy Materials, 2018, 8, 1801155.	10.2	34
80	Phase Directing Ability of an Ionic Liquid Solvent for the Synthesis of HER-Active Ni <sub>2</sub> P Nanocrystals. ACS Applied Energy Materials, 2018, 1, 1823-1827.	2.5	30
81	Template-Free Synthesis of Periodic Three-Dimensional PbSe Nanostructures via Photoelectrodeposition. Journal of the American Chemical Society, 2018, 140, 6536-6539.	6.6	14
82	Reduction of Aqueous CO <sub>2</sub> to 1-Propanol at MoS <sub>2</sub> Electrodes. Chemistry of Materials, 2018, 30, 4902-4908.	3.2	73
83	Optically Manipulated Bottom-up Growth of Nanopatterned Semiconductor Films. ECS Meeting Abstracts, 2018, , .	0.0	0
84	Highly Directional Deposition of Oriented Nanoscale Semiconductor Structures with Phototropic Control. ECS Meeting Abstracts, 2018, , .	0.0	0
85	A Mechanistic Study of the Oxidative Reaction of Hydrogen-Terminated Si(111) Surfaces with Liquid Methanol. Journal of Physical Chemistry C, 2017, 121, 4270-4282.	1.5	16
86	Excitonic Effects in Emerging Photovoltaic Materials: A Case Study in Cu <sub>2</sub> 0. ACS Energy Letters, 2017, 2, 431-437.	8.8	28
87	A comparison of the chemical, optical and electrocatalytic properties of water-oxidation catalysts for use in integrated solar-fuel generators. Energy and Environmental Science, 2017, 10, 987-1002.	15.6	50
88	Evaluation of flow schemes for near-neutral pH electrolytes in solar-fuel generators. Sustainable Energy and Fuels, 2017, 1, 458-466.	2.5	36
89	Membranes for artificial photosynthesis. Energy and Environmental Science, 2017, 10, 1320-1338.	15.6	65
90	Nanoelectrical and Nanoelectrochemical Imaging of Pt/p‣i and Pt/p <sup>+</sup> ‣i Electrodes. ChemSusChem, 2017, 10, 4657-4663.	3.6	13

#	Article	IF	CITATIONS
91	Porous Nanomaterials: Porous Nanomaterials for Ultrabroadband Omnidirectional Antiâ€Reflection Surfaces with Applications in High Concentration Photovoltaics (Adv. Energy Mater. 7/2017). Advanced Energy Materials, 2017, 7, .	10.2	2
92	Operando X-ray photoelectron spectroscopic investigations of the electrochemical double layer at Ir/KOH(aq) interfaces. Journal of Electron Spectroscopy and Related Phenomena, 2017, 221, 99-105.	0.8	10
93	Porous Nanomaterials for Ultrabroadband Omnidirectional Antiâ€Reflection Surfaces with Applications in High Concentration Photovoltaics. Advanced Energy Materials, 2017, 7, 1601992.	10.2	27
94	<i>Operando</i> Spectroscopic Analysis of CoP Films Electrocatalyzing the Hydrogen-Evolution Reaction. Journal of the American Chemical Society, 2017, 139, 12927-12930.	6.6	127
95	Growth of Epitaxial ZnSnxGe1â^'xN2 Alloys by MBE. Scientific Reports, 2017, 7, 11990.	1.6	8
96	Comparative Study in Acidic and Alkaline Media of the Effects of pH and Crystallinity on the Hydrogen-Evolution Reaction on MoS <sub>2</sub> and MoSe <sub>2</sub> . ACS Energy Letters, 2017, 2, 2234-2238.	8.8	78
97	Vibrational Sum-Frequency Spectroscopic Investigation of the Structure and Azimuthal Anisotropy of Propynyl-Terminated Si(111) Surfaces. Journal of Physical Chemistry C, 2017, 121, 16872-16878.	1.5	6
98	Machine-Learning Methods Enable Exhaustive Searches for Active Bimetallic Facets and Reveal Active Site Motifs for CO <sub>2</sub> Reduction. ACS Catalysis, 2017, 7, 6600-6608.	5.5	300
99	Crystalline nickel manganese antimonate as a stable water-oxidation catalyst in aqueous 1.0 M H <sub>2</sub> SO <sub>4</sub> . Energy and Environmental Science, 2017, 10, 2103-2108.	15.6	158
100	Photoelectrochemical Behavior of a Molecular Ru-Based Water-Oxidation Catalyst Bound to TiO <sub>2</sub> -Protected Si Photoanodes. Journal of the American Chemical Society, 2017, 139, 11345-11348.	6.6	56
101	Effects of surface condition on the work function and valence-band position of ZnSnN2. Applied Physics A: Materials Science and Processing, 2017, 123, 1.	1.1	17
102	Oxidant-Activated Reactions of Nucleophiles with Silicon Nanocrystals. Chemistry of Materials, 2017, 29, 7002-7013.	3.2	2
103	Experimental and theoretical study of rotationally inelastic diffraction of H2(D2) from methyl-terminated Si(111). Journal of Chemical Physics, 2016, 145, 084705.	1.2	3
104	Developing a scalable artificial photosynthesis technology through nanomaterials by design. Nature Nanotechnology, 2016, 11, 1010-1019.	15.6	162
105	A comparative technoeconomic analysis of renewable hydrogen production using solar energy. Energy and Environmental Science, 2016, 9, 2354-2371.	15.6	688
106	Morphological Expression of the Coherence and Relative Phase of Optical Inputs to the Photoelectrodeposition of Nanopatterned Se–Te Films. Nano Letters, 2016, 16, 2963-2968.	4.5	16
107	Progress Towards a Synergistically Integrated, Scalable Solar Fuels Generator. ACS Symposium Series, 2016, , 3-22.	0.5	0
108	Enhanced Absorption and <1% Spectrum-and-Angle-Averaged Reflection in Tapered Microwire Arrays. ACS Photonics, 2016, 3, 1854-1861.	3.2	24

#	Article	IF	CITATIONS
109	Synthesis, Characterization, and Properties of Metal Phosphide Catalysts for the Hydrogen-Evolution Reaction. Chemistry of Materials, 2016, 28, 6017-6044.	3.2	519
110	Modellierung, Simulation und Implementierung von Zellen für die solargetriebene Wasserspaltung. Angewandte Chemie, 2016, 128, 13168-13183.	1.6	10
111	Solar-Driven Reduction of 1 atm of CO <sub>2</sub> to Formate at 10% Energy-Conversion Efficiency by Use of a TiO <sub>2</sub> -Protected Ill–V Tandem Photoanode in Conjunction with a Bipolar Membrane and a Pd/C Cathode. ACS Energy Letters, 2016, 1, 764-770.	8.8	173
112	Solarâ€Driven Water Splitting: A Stabilized, Intrinsically Safe, 10% Efficient, Solarâ€Driven Waterâ€Splitting Cell Incorporating Earthâ€Abundant Electrocatalysts with Steadyâ€State pH Gradients and Product Separation Enabled by a Bipolar Membrane (Adv. Energy Mater. 13/2016). Advanced Energy Materials, 2016, 6, .	10.2	5
113	Modeling, Simulation, and Implementation of Solarâ€Driven Waterâ€Splitting Devices. Angewandte Chemie - International Edition, 2016, 55, 12974-12988.	7.2	119
114	Control of the Band-Edge Positions of Crystalline Si(111) by Surface Functionalization with 3,4,5-Trifluorophenylacetylenyl Moieties. Journal of Physical Chemistry C, 2016, 120, 14157-14169.	1.5	34
115	Operando Analyses of Solar Fuels Light Absorbers and Catalysts. Electrochimica Acta, 2016, 211, 711-719.	2.6	23
116	Lightly Fluorinated Graphene as a Protective Layer for n-Type Si(111) Photoanodes in Aqueous Electrolytes. Nano Letters, 2016, 16, 4082-4086.	4.5	19
117	Aspects of science and technology in support of legal and policy frameworks associated with a global carbon emissions-control regime. Energy and Environmental Science, 2016, 9, 2172-2176.	15.6	41
118	Profiling Photoinduced Carrier Generation in Semiconductor Microwire Arrays via Photoelectrochemical Metal Deposition. Nano Letters, 2016, 16, 5015-5021.	4.5	15
119	Modeling and Simulation of the Spatial and Light-Intensity Dependence of Product Distributions in an Integrated Photoelectrochemical CO <sub>2</sub> Reduction System. ACS Energy Letters, 2016, 1, 273-280.	8.8	24
120	A Stabilized, Intrinsically Safe, 10% Efficient, Solarâ€Driven Waterâ€Splitting Cell Incorporating Earthâ€Abundant Electrocatalysts with Steadyâ€State pH Gradients and Product Separation Enabled by a Bipolar Membrane. Advanced Energy Materials, 2016, 6, 1600379.	10.2	114
121	Si/TiO <sub>2</sub> Tandem-Junction Microwire Arrays for Unassisted Solar-Driven Water Splitting. Journal of the Electrochemical Society, 2016, 163, H261-H264.	1.3	25
122	Research opportunities to advance solar energy utilization. Science, 2016, 351, aad1920.	6.0	1,480
123	An Electrochemical, Microtopographical and Ambient Pressure X-Ray Photoelectron Spectroscopic Investigation of Si/TiO <sub>2</sub> /Ni/Electrolyte Interfaces. Journal of the Electrochemical Society, 2016, 163, H139-H146.	1.3	24
124	Photoelectrochemical Behavior of n-Type GaAs(100) Electrodes Coated by a Single Layer of Graphene. Journal of Physical Chemistry C, 2016, 120, 6989-6995.	1.5	22
125	Principles and implementations of electrolysis systems for water splitting. Materials Horizons, 2016, 3, 169-173.	6.4	202
126	Nickel–Gallium-Catalyzed Electrochemical Reduction of CO <sub>2</sub> to Highly Reduced Products at Low Overpotentials. ACS Catalysis, 2016, 6, 2100-2104.	5.5	238

#	Article	IF	CITATIONS
127	Electrical, Photoelectrochemical, and Photoelectron Spectroscopic Investigation of the Interfacial Transport and Energetics of Amorphous TiO <sub>2</sub> /Si Heterojunctions. Journal of Physical Chemistry C, 2016, 120, 3117-3129.	1.5	77
128	570 mV photovoltage, stabilized n-Si/CoO <sub>x</sub> heterojunction photoanodes fabricated using atomic layer deposition. Energy and Environmental Science, 2016, 9, 892-897.	15.6	137
129	Polarization Control of Morphological Pattern Orientation During Light-Mediated Synthesis of Nanostructured Se–Te Films. ACS Nano, 2016, 10, 102-111.	7.3	17
130	Protection of inorganic semiconductors for sustained, efficient photoelectrochemical water oxidation. Catalysis Today, 2016, 262, 11-23.	2.2	87
131	A scanning probe investigation of the role of surface motifs in the behavior of p-WSe <sub>2</sub> photocathodes. Energy and Environmental Science, 2016, 9, 164-175.	15.6	33
132	Semiconducting ZnSnxGe1â^'xN2 alloys prepared by reactive radio-frequency sputtering. APL Materials, 2015, 3, 076104.	2.2	16
133	Direct observation of the energetics at a semiconductor/liquid junction by operando X-ray photoelectron spectroscopy. Energy and Environmental Science, 2015, 8, 2409-2416.	15.6	149
134	Electrical Characteristics of the Junction between PEDOT:PSS and Thiophene-Functionalized Silicon Microwires. ACS Applied Materials & amp; Interfaces, 2015, 7, 27160-27166.	4.0	18
135	Modeling, Simulation, and Fabrication of a Fully Integrated, Acidâ€stable, Scalable Solarâ€Driven Waterâ€Splitting System. ChemSusChem, 2015, 8, 544-551.	3.6	89
136	Microwave Near-Field Imaging of Two-Dimensional Semiconductors. Nano Letters, 2015, 15, 1122-1127.	4.5	42
137	Use of Mixed CH <sub>3</sub> –/HC(O)CH <sub>2</sub> CH <sub>2</sub> –Si(111) Functionality to Control Interfacial Chemical and Electronic Properties During the Atomic-Layer Deposition of Ultrathin Oxides on Si(111). Journal of Physical Chemistry Letters, 2015, 6, 722-726.	2.1	19
138	Ordered Silicon Microwire Arrays Grown from Substrates Patterned Using Imprint Lithography and Electrodeposition. ACS Applied Materials & amp; Interfaces, 2015, 7, 1396-1400.	4.0	6
139	Stable Solar-Driven Water Oxidation to O <sub>2</sub> (g) by Ni-Oxide-Coated Silicon Photoanodes. Journal of Physical Chemistry Letters, 2015, 6, 592-598.	2.1	144
140	Highly branched cobalt phosphide nanostructures for hydrogen-evolution electrocatalysis. Journal of Materials Chemistry A, 2015, 3, 5420-5425.	5.2	116
141	Stable solar-driven oxidation of water by semiconducting photoanodes protected by transparent catalytic nickel oxide films. Proceedings of the National Academy of Sciences of the United States of America, 2015, 112, 3612-3617.	3.3	180
142	Methods of photoelectrode characterization with high spatial and temporal resolution. Energy and Environmental Science, 2015, 8, 2863-2885.	15.6	51
143	Functional integration of Ni–Mo electrocatalysts with Si microwire array photocathodes to simultaneously achieve high fill factors and light-limited photocurrent densities for solar-driven hydrogen evolution. Energy and Environmental Science, 2015, 8, 2977-2984.	15.6	60
144	Synthesis and Characterization of Atomically Flat Methyl-Terminated Ge(111) Surfaces. Journal of the American Chemical Society, 2015, 137, 9006-9014.	6.6	18

#	Article	IF	CITATIONS
145	The Influence of Structure and Processing on the Behavior of TiO <sub>2</sub> Protective Layers for Stabilization of n-Si/TiO <sub>2</sub> /Ni Photoanodes for Water Oxidation. ACS Applied Materials & Interfaces, 2015, 7, 15189-15199.	4.0	114
146	Interface engineering of the photoelectrochemical performance of Ni-oxide-coated n-Si photoanodes by atomic-layer deposition of ultrathin films of cobalt oxide. Energy and Environmental Science, 2015, 8, 2644-2649.	15.6	130
147	Synthesis, Characterization, and Reactivity of Ethynyl- and Propynyl-Terminated Si(111) Surfaces. Journal of Physical Chemistry C, 2015, 119, 19847-19862.	1.5	26
148	An electrochemical engineering assessment of the operational conditions and constraints for solar-driven water-splitting systems at near-neutral pH. Energy and Environmental Science, 2015, 8, 2760-2767.	15.6	82
149	Tailoring of Interfacial Mechanical Shear Strength by Surface Chemical Modification of Silicon Microwires Embedded in Nafion Membranes. ACS Nano, 2015, 9, 5143-5153.	7.3	18
150	Comparison of the Performance of CoP-Coated and Pt-Coated Radial Junction n <sup>+</sup> p-Silicon Microwire-Array Photocathodes for the Sunlight-Driven Reduction of Water to H <sub>2</sub> (g). Journal of Physical Chemistry Letters, 2015, 6, 1679-1683.	2.1	60
151	Sputtered NiO <i><sub>x</sub></i> Films for Stabilization of p <sup>+</sup> nâ€InP Photoanodes for Solarâ€Đriven Water Oxidation. Advanced Energy Materials, 2015, 5, 1402276.	10.2	71
152	A quantitative analysis of the efficiency of solar-driven water-splitting device designs based on tandem photoabsorbers patterned with islands of metallic electrocatalysts. Energy and Environmental Science, 2015, 8, 1736-1747.	15.6	66
153	Unassisted solar-driven photoelectrosynthetic HI splitting using membrane-embedded Si microwire arrays. Energy and Environmental Science, 2015, 8, 1484-1492.	15.6	35
154	Methods for comparing the performance of energy-conversion systems for use in solar fuels and solar electricity generation. Energy and Environmental Science, 2015, 8, 2886-2901.	15.6	196
155	Self-Optimizing Photoelectrochemical Growth of Nanopatterned Se–Te Films in Response to the Spectral Distribution of Incident Illumination. Nano Letters, 2015, 15, 7071-7076.	4.5	19
156	Vibrational dynamics and band structure of methyl-terminated Ge(111). Journal of Chemical Physics, 2015, 143, 124705.	1.2	3
157	Thin-Film Materials for the Protection of Semiconducting Photoelectrodes in Solar-Fuel Generators. Journal of Physical Chemistry C, 2015, 119, 24201-24228.	1.5	245
158	Enhancement of the performance of GaP solar cells by embedded In(N)P quantum dots. Nano Energy, 2015, 15, 782-788.	8.2	3
159	Operational constraints and strategies for systems to effect the sustainable, solar-driven reduction of atmospheric CO <sub>2</sub> . Energy and Environmental Science, 2015, 8, 3663-3674.	15.6	52
160	A monolithically integrated, intrinsically safe, 10% efficient, solar-driven water-splitting system based on active, stable earth-abundant electrocatalysts in conjunction with tandem Ill–V light absorbers protected by amorphous TiO <sub>2</sub> films. Energy and Environmental Science, 2015, 8, 3166-3172.	15.6	263
161	A sensitivity analysis to assess the relative importance of improvements in electrocatalysts, light absorbers, and system geometry on the efficiency of solar-fuels generators. Energy and Environmental Science, 2015, 8, 876-886.	15.6	32
162	A taxonomy for solar fuels generators. Energy and Environmental Science, 2015, 8, 16-25.	15.6	170

#	Article	IF	CITATIONS
163	Electrochemical surface science twenty years later: Expeditions into the electrocatalysis of reactions at the core of artificial photosynthesis. Surface Science, 2015, 631, 285-294.	0.8	22
164	Stabilization of Si microwire arrays for solar-driven H <sub>2</sub> 0 oxidation to O <sub>2</sub> (g) in 1.0 M KOH(aq) using conformal coatings of amorphous TiO <sub>2</sub> . Energy and Environmental Science, 2015, 8, 203-207.	15.6	128
165	Solar energy conversion via hot electron internal photoemission in metallic nanostructures: Efficiency estimates. Journal of Applied Physics, 2014, 115, .	1.1	126
166	The interaction of organic adsorbate vibrations with substrate lattice waves in methyl-Si(111)-(1 × 1). Journal of Chemical Physics, 2014, 141, 024702.	1.2	8
167	What a Difference a Bond Makes: The Structural, Chemical, and Physical Properties of Methyl-Terminated Si(111) Surfaces. Accounts of Chemical Research, 2014, 47, 3037-3044.	7.6	75
168	Comparison between the measured and modeled hydrogen-evolution activity of Ni- or Pt-coated silicon photocathodes. International Journal of Hydrogen Energy, 2014, 39, 16220-16226.	3.8	13
169	Will Solar-Driven Water-Splitting Devices See the Light of Day?. Chemistry of Materials, 2014, 26, 407-414.	3.2	654
170	Highly Active Electrocatalysis of the Hydrogen Evolution Reaction by Cobalt Phosphide Nanoparticles. Angewandte Chemie - International Edition, 2014, 53, 5427-5430.	7.2	1,033
171	Synthesis and hydrogen-evolution activity of tungsten selenide thin films deposited on tungsten foils. Journal of Electroanalytical Chemistry, 2014, 716, 45-48.	1.9	51
172	Amorphous TiO <sub>2</sub> coatings stabilize Si, GaAs, and GaP photoanodes for efficient water oxidation. Science, 2014, 344, 1005-1009.	6.0	1,189
173	Silicon Microwire Arrays for Solar Energy-Conversion Applications. Journal of Physical Chemistry C, 2014, 118, 747-759.	1.5	85
174	Measurement of the Electrical Resistance of n-Type Si Microwire/p-Type Conducting Polymer Junctions for Use in Artificial Photosynthesis. Journal of Physical Chemistry C, 2014, 118, 27742-27748.	1.5	9
175	An experimental and modeling/simulation-based evaluation of the efficiency and operational performance characteristics of an integrated, membrane-free, neutral pH solar-driven water-splitting system. Energy and Environmental Science, 2014, 7, 3371-3380.	15.6	152
176	CoP as an Acid-Stable Active Electrocatalyst for the Hydrogen-Evolution Reaction: Electrochemical Synthesis, Interfacial Characterization and Performance Evaluation. Journal of Physical Chemistry C, 2014, 118, 29294-29300.	1.5	216
177	Assembly, characterization, and electrochemical properties of immobilized metal bipyridyl complexes on silicon(111) surfaces. Dalton Transactions, 2014, 43, 15004-15012.	1.6	33
178	Stabilization of n-cadmium telluride photoanodes for water oxidation to O <sub>2</sub> (g) in aqueous alkaline electrolytes using amorphous TiO <sub>2</sub> films formed by atomic-layer deposition. Energy and Environmental Science, 2014, 7, 3334-3337.	15.6	111
179	Two stories from the ISACS 12 conference: solar-fuel devices and catalyst identification. Energy and Environmental Science, 2014, 7, 1207-1211.	15.6	12
180	Use of Bipolar Membranes for Maintaining Steady‧tate pH Gradients in Membrane‧upported, Solarâ€Driven Water Splitting. ChemSusChem, 2014, 7, 3021-3027.	3.6	107

#	Article	IF	CITATIONS
181	<i>Operando</i> Synthesis of Macroporous Molybdenum Diselenide Films for Electrocatalysis of the Hydrogen-Evolution Reaction. ACS Catalysis, 2014, 4, 2866-2873.	5.5	122
182	Measurement of minority-carrier diffusion lengths using wedge-shaped semiconductor photoelectrodes. Energy and Environmental Science, 2014, 7, 3424-3430.	15.6	63
183	Electrocatalytic hydrogen evolution using amorphous tungsten phosphide nanoparticles. Chemical Communications, 2014, 50, 11026.	2.2	264
184	Low Temperature Solution-Phase Deposition of SnS Thin Films. Chemistry of Materials, 2014, 26, 5444-5446.	3.2	84
185	Electrocatalytic and Photocatalytic Hydrogen Production from Acidic and Neutral-pH Aqueous Solutions Using Iron Phosphide Nanoparticles. ACS Nano, 2014, 8, 11101-11107.	7.3	429
186	Cellular uptake and cytotoxicity of a near-IR fluorescent corrole–TiO2 nanoconjugate. Journal of Inorganic Biochemistry, 2014, 140, 39-44.	1.5	16
187	Modeling the Performance of an Integrated Photoelectrolysis System with 10 × Solar Concentrators. Journal of the Electrochemical Society, 2014, 161, F1101-F1110.	1.3	36
188	Electrocatalysis of the hydrogen-evolution reaction by electrodeposited amorphous cobalt selenide films. Journal of Materials Chemistry A, 2014, 2, 13835-13839.	5.2	133
189	Photoelectrochemistry of core–shell tandem junction n–p <sup>+</sup> -Si/n-WO <sub>3</sub> microwire array photoelectrodes. Energy and Environmental Science, 2014, 7, 779-790.	15.6	152
190	Amorphous Molybdenum Phosphide Nanoparticles for Electrocatalytic Hydrogen Evolution. Chemistry of Materials, 2014, 26, 4826-4831.	3.2	379
191	Improved Stability of Polycrystalline Bismuth Vanadate Photoanodes by Use of Dual-Layer Thin TiO <sub>2</sub> /Ni Coatings. Journal of Physical Chemistry C, 2014, 118, 19618-19624.	1.5	129
192	An analysis of the optimal band gaps of light absorbers in integrated tandem photoelectrochemical water-splitting systems. Energy and Environmental Science, 2013, 6, 2984.	15.6	497
193	Optical, electrical, and solar energy-conversion properties of gallium arsenide nanowire-array photoanodes. Energy and Environmental Science, 2013, 6, 1879.	15.6	102
194	Photoelectrochemical oxidation of anions by WO3 in aqueous and nonaqueous electrolytes. Energy and Environmental Science, 2013, 6, 2646.	15.6	57
195	Photoelectrochemical Behavior of n-type Si(100) Electrodes Coated with Thin Films of Manganese Oxide Grown by Atomic Layer Deposition. Journal of Physical Chemistry C, 2013, 117, 4931-4936.	1.5	137
196	Photoelectrochemical Behavior of n-Type Si(111) Electrodes Coated With a Single Layer of Graphene. Journal of the American Chemical Society, 2013, 135, 17246-17249.	6.6	53
197	Redox Properties of Mixed Methyl/Vinylferrocenyl Monolayers on Si(111) Surfaces. Journal of Physical Chemistry C, 2013, 117, 27012-27022.	1.5	29
198	Measurement of the Band Bending and Surface Dipole at Chemically Functionalized Si(111)/Vacuum Interfaces. Journal of Physical Chemistry C, 2013, 117, 18031-18042.	1.5	85

4

#	Article	IF	CITATIONS
199	Electrical Junction Behavior of Poly(3,4-ethylenedioxythiophene) (PEDOT) Contacts to H-Terminated and CH <sub>3</sub> -Terminated p-, n-, and n <sup>+</sup> -Si(111) Surfaces. Journal of Physical Chemistry C, 2013, 117, 14485-14492.	1.5	22
200	Simulations of the irradiation and temperature dependence of the efficiency of tandem photoelectrochemical water-splitting systems. Energy and Environmental Science, 2013, 6, 3605.	15.6	148
201	Modeling an integrated photoelectrolysis system sustained by water vapor. Energy and Environmental Science, 2013, 6, 3713.	15.6	52
202	Hydrogen Evolution from Pt/Ru-Coated p-Type WSe <sub>2</sub> Photocathodes. Journal of the American Chemical Society, 2013, 135, 223-231.	6.6	192
203	Ni–Mo Nanopowders for Efficient Electrochemical Hydrogen Evolution. ACS Catalysis, 2013, 3, 166-169.	5.5	725
204	Detection of ammonia, 2,4,6-trinitrotoluene, and common organic vapors using thin-film carbon black-metalloporphyrin composite chemiresistors. Sensors and Actuators B: Chemical, 2013, 188, 761-767.	4.0	16
205	Hybridization of Surface Waves with Organic Adlayer Librations: A Helium Atom Scattering and Density Functional Perturbation Theory Study of Methyl-Si(111). Physical Review Letters, 2013, 110, 156102.	2.9	13
206	Nanostructured Nickel Phosphide as an Electrocatalyst for the Hydrogen Evolution Reaction. Journal of the American Chemical Society, 2013, 135, 9267-9270.	6.6	2,624
207	Heck Coupling of Olefins to Mixed Methyl/Thienyl Monolayers on Si(111) Surfaces. Journal of the American Chemical Society, 2013, 135, 10081-10090.	6.6	49
208	Vibrational Sum Frequency Spectroscopic Investigation of the Azimuthal Anisotropy and Rotational Dynamics of Methyl-Terminated Silicon(111) Surfaces. Journal of Physical Chemistry C, 2013, 117, 935-944.	1.5	41
209	Enhanced Stability and Activity for Water Oxidation in Alkaline Media with Bismuth Vanadate Photoelectrodes Modified with a Cobalt Oxide Catalytic Layer Produced by Atomic Layer Deposition. Journal of Physical Chemistry Letters, 2013, 4, 4188-4191.	2.1	116
210	Combined Theoretical and Experimental Study of Band-Edge Control of Si through Surface Functionalization. Journal of Physical Chemistry C, 2013, 117, 5188-5194.	1.5	57
211	Phototropic growth control of nanoscale pattern formation in photoelectrodeposited Se-Te films. Proceedings of the National Academy of Sciences of the United States of America, 2013, 110, 19707-19712.	3.3	25
212	Modeling, simulation, and design criteria for photoelectrochemical water-splitting systems. Energy and Environmental Science, 2012, 5, 9922.	15.6	264
213	Wafer-Scale Growth of Silicon Microwire Arrays for Photovoltaics and Solar Fuel Generation. IEEE Journal of Photovoltaics, 2012, 2, 294-297.	1.5	15
214	Magnetic Field Alignment of Randomly Oriented, High Aspect Ratio Silicon Microwires into Vertically Oriented Arrays. ACS Nano, 2012, 6, 10303-10310.	7.3	17
215	Photoanodic behavior of vapor-liquid-solid–grown, lightly doped, crystalline Si microwire arrays. Energy and Environmental Science, 2012, 5, 6867.	15.6	29

Photoelectrochemical characterization of Si microwire array solar cells., 2012,,.

#	Article	IF	CITATIONS
217	Comparison between the electrical junction properties of H-terminated and methyl-terminated individual Si microwire/polymer assemblies for photoelectrochemical fuel production. Energy and Environmental Science, 2012, 5, 9789.	15.6	18
218	Comparison of the Photoelectrochemical Behavior of H-Terminated and Methyl-Terminated Si(111) Surfaces in Contact with a Series of One-Electron, Outer-Sphere Redox Couples in CH <sub>3</sub> CN. Journal of Physical Chemistry C, 2012, 116, 23569-23576.	1.5	64
219	A quantitative assessment of the competition between water and anion oxidation at WO3 photoanodes in acidic aqueous electrolytes. Energy and Environmental Science, 2012, 5, 5694.	15.6	273
220	Hydrogen-evolution characteristics of Ni–Mo-coated, radial junction, n+p-silicon microwire array photocathodes. Energy and Environmental Science, 2012, 5, 9653.	15.6	182
221	In Situ Nanomechanical Measurements of Interfacial Strength in Membrane-Embedded Chemically Functionalized Si Microwires for Flexible Solar Cells. Nano Letters, 2012, 12, 3296-3301.	4.5	10
222	Photoelectrochemical Behavior of Planar and Microwireâ€Array Si GaP Electrodes. Advanced Energy Materials, 2012, 2, 1109-1116.	10.2	39
223	820 mV open-circuit voltages from Cu2O/CH3CN junctions. Energy and Environmental Science, 2011, 4, 1311.	15.6	87
224	Proton exchange membrane electrolysis sustained by water vapor. Energy and Environmental Science, 2011, 4, 2993.	15.6	109
225	Characterization of the Electrical Properties of Individual p-Si Microwire/Polymer/n-Si Microwire Assemblies. Journal of Physical Chemistry C, 2011, 115, 24945-24950.	1.5	15
226	High-performance Si microwire photovoltaics. Energy and Environmental Science, 2011, 4, 866.	15.6	196
227	Electrical Characterization of Si Microwires and of Si Microwire/Conducting Polymer Composite Junctions. Journal of Physical Chemistry Letters, 2011, 2, 675-680.	2.1	17
228	Response and Discrimination Performance of Arrays of Organothiol-Capped Au Nanoparticle Chemiresistive Vapor Sensors. Journal of Physical Chemistry C, 2011, 115, 6208-6217.	1.5	27
229	Control of the pH-Dependence of the Band Edges of Si(111) Surfaces Using Mixed Methyl/Allyl Monolayers. Journal of Physical Chemistry C, 2011, 115, 8594-8601.	1.5	33
230	Photoelectrochemical Hydrogen Evolution Using Si Microwire Arrays. Journal of the American Chemical Society, 2011, 133, 1216-1219.	6.6	561
231	pH-Independent, 520 mV Open-Circuit Voltages of Si/Methyl Viologen <sup>2+/+</sup> Contacts Through Use of Radial n <sup>+</sup> p-Si Junction Microwire Array Photoelectrodes. Journal of Physical Chemistry C, 2011, 115, 594-598.	1.5	52
232	Evaluation of Pt, Ni, and Ni–Mo electrocatalysts for hydrogen evolution on crystalline Si electrodes. Energy and Environmental Science, 2011, 4, 3573.	15.6	440
233	Designing electronic/ionic conducting membranes for artificial photosynthesis. Energy and Environmental Science, 2011, 4, 1700.	15.6	53
234	Electrical conductivity, ionic conductivity, optical absorption, and gas separation properties of ionically conductive polymer membranes embedded with Si microwire arrays. Energy and Environmental Science, 2011, 4, 1772.	15.6	103

#	Article	IF	CITATIONS
235	Composites of carboxylate-capped TiO2 nanoparticles and carbon black as chemiresistive vapor sensors. Sensors and Actuators B: Chemical, 2011, 158, 17-22.	4.0	9
236	Wafer-scale growth of silicon microwire arrays for photovoltaics. , 2011, , .		1
237	Solar Water Splitting Cells. Chemical Reviews, 2010, 110, 6446-6473.	23.0	8,307
238	Flexible, Polymerâ€Supported, Si Wire Array Photoelectrodes. Advanced Materials, 2010, 22, 3277-3281.	11.1	85
239	Enhanced absorption and carrier collection in Si wire arrays for photovoltaic applications. Nature Materials, 2010, 9, 239-244.	13.3	1,085
240	Hexathiapentacene Nanowires as Chemical Vapor Sensors. Materials Research Society Symposia Proceedings, 2010, 1253, 8.	0.1	0
241	Photoelectrochemical water splitting: silicon photocathodes for hydrogen evolution. , 2010, , .		11
242	Energy-Conversion Properties of Vapor-Liquid-Solid–Grown Silicon Wire-Array Photocathodes. Science, 2010, 327, 185-187.	6.0	489
243	Helium atom diffraction measurements of the surface structure and vibrational dynamics of CH3–Si(111) and CD3–Si(111) surfaces. Journal of Chemical Physics, 2010, 133, 104705.	1.2	29
244	Synthesis and Characterization of Mixed Methyl/Allyl Monolayers on Si(111). Journal of Physical Chemistry B, 2010, 114, 14298-14302.	1.2	55
245	Response versus Chain Length of Alkanethiol-Capped Au Nanoparticle Chemiresistive Chemical Vapor Sensors. Journal of Physical Chemistry C, 2010, 114, 21914-21920.	1.5	43
246	Si microwire-array solar cells. Energy and Environmental Science, 2010, 3, 1037.	15.6	217
247	10 â€, μ m minority-carrier diffusion lengths in Si wires synthesized by Cu-catalyzed vapor-liquid-solid growth. Applied Physics Letters, 2009, 95, .	1.5	84
248	Behavior of Electrodeposited Cd and Pb Schottky Junctions on CH[sub 3]-Terminated n-Si(111) Surfaces. Journal of the Electrochemical Society, 2009, 156, H123.	1.3	17
249	Flexible Polymerâ€Embedded Si Wire Arrays. Advanced Materials, 2009, 21, 325-328.	11.1	144
250	A Perspective on Forward Research and Development Paths for Cost-Effective Solar Energy Utilization. ChemSusChem, 2009, 2, 383-386.	3.6	23
251	Infrared Vibrational Spectroscopy of Isotopically Labeled Ethyl-Terminated Si(111) Surfaces Prepared Using a Two-Step Chlorination/Alkylation Procedure. Journal of Physical Chemistry C, 2009, 113, 15239-15245.	1.5	28
252	Combinatorial synthesis and high-throughput photopotential and photocurrent screening of mixed-metal oxides for photoelectrochemical water splitting. Energy and Environmental Science, 2009, 2, 103-112.	15.6	87

#	Article	IF	CITATIONS
253	Detection of organic vapors and NH3(g) using thin-film carbon black–metallophthalocyanine composite chemiresistors. Sensors and Actuators B: Chemical, 2008, 134, 521-531.	4.0	34
254	Photovoltaic Measurements in Single-Nanowire Silicon Solar Cells. Nano Letters, 2008, 8, 710-714.	4.5	550
255	SEMICONDUCTOR/LIQUID JUNCTION PHOTOELECTROCHEMICAL SOLAR CELLS. Series on Photoconversion of Solar Energy, 2008, , 537-589.	0.2	2
256	The Role of Band Bending in Affecting the Surface Recombination Velocities for Si(111) in Contact with Aqueous Acidic Electrolytes. Journal of Physical Chemistry C, 2008, 112, 5911-5921.	1.5	23
257	Near-Ideal Photodiodes from Sintered Gold Nanoparticle Films on Methyl-Terminated Si(111) Surfaces. Journal of the American Chemical Society, 2008, 130, 3300-3301.	6.6	49
258	A Comparison Between the Behavior of Nanorod Array and Planar Cd(Se, Te) Photoelectrodes. Journal of Physical Chemistry C, 2008, 112, 6186-6193.	1.5	122
259	Phosphine Functionalization of GaAs(111)A Surfaces. Journal of Physical Chemistry C, 2008, 112, 18467-18473.	1.5	13
260	Repeated epitaxial growth and transfer of arrays of patterned, vertically aligned, crystalline Si wires from a single Si(111) substrate. Applied Physics Letters, 2008, 93, .	1.5	71
261	Extraction of spatiotemporal response information from sorption-based cross-reactive sensor arrays for the identification and quantification of analyte mixtures. Proceedings of SPIE, 2008, , .	0.8	0
262	Solar energy conversion. Physics Today, 2007, 60, 37-42.	0.3	484
263	Use of Spatiotemporal Response Information from Sorption-Based Sensor Arrays to Identify and Quantify the Composition of Analyte Mixtures. Langmuir, 2007, 23, 13232-13241.	1.6	29
264	Electrical Properties of Junctions between Hg and Si(111) Surfaces Functionalized with Short-Chain Alkylsâ€. Journal of Physical Chemistry C, 2007, 111, 17690-17699.	1.5	78
265	High-Resolution Synchrotron Photoemission Studies of the Electronic Structure and Thermal Stability of CH <sub>3</sub> - and C <sub>2</sub> H <sub>5</sub> -Functionalized Si(111) Surfaces. Journal of Physical Chemistry C, 2007, 111, 18204-18213.	1.5	42
266	High Aspect Ratio Silicon Wire Array Photoelectrochemical Cells. Journal of the American Chemical Society, 2007, 129, 12346-12347.	6.6	240
267	Principles and Applications of Semiconductor Photoelectrochemistry. Progress in Inorganic Chemistry, 2007, , 21-144.	3.0	130
268	Growth of vertically aligned Si wire arrays over large areas (>1cm2) with Au and Cu catalysts. Applied Physics Letters, 2007, 91, .	1.5	274
269	Near-Surface Channel Impedance Measurements, Open-Circuit Impedance Spectra, and Differential Capacitance vs Potential Measurements of the Fermi Level Position at Si/CH3CN Contacts. Journal of Physical Chemistry C, 2007, 111, 8120-8127.	1.5	7
270	Toward Cost-Effective Solar Energy Use. Science, 2007, 315, 798-801.	6.0	2,109

#	Article	IF	CITATIONS
271	Vapor Sensing Using Polymer/Carbon Black Composites in the Percolative Conduction Regime. Langmuir, 2006, 22, 7928-7935.	1.6	50
272	Scanning tunneling spectroscopy of methyl- and ethyl-terminated Si(111) surfaces. Applied Physics Letters, 2006, 88, 252111.	1.5	44
273	Electrical Characteristics and Chemical Stability of Non-Oxidized, Methyl-Terminated Silicon Nanowires. Journal of the American Chemical Society, 2006, 128, 8990-8991.	6.6	142
274	Quantum Mechanics Calculations of the Thermodynamically Controlled Coverage and Structure of Alkyl Monolayers on Si(111) Surfaces. Journal of Physical Chemistry B, 2006, 110, 14842-14848.	1.2	32
275	High-Resolution X-ray Photoelectron Spectroscopy of Chlorine-Terminated GaAs(111)A Surfaces. Journal of Physical Chemistry B, 2006, 110, 15641-15644.	1.2	17
276	Infrared Spectroscopic Investigation of the Reaction of Hydrogen-Terminated, (111)-Oriented, Silicon Surfaces with Liquid Methanol. Journal of Physical Chemistry B, 2006, 110, 20426-20434.	1.2	64
277	Transmission Infrared Spectroscopy of Methyl- and Ethyl-Terminated Silicon(111) Surfaces. Journal of Physical Chemistry B, 2006, 110, 7349-7356.	1.2	80
278	Chemiresistors for Array-Based Vapor Sensing Using Composites of Carbon Black with Low Volatility Organic Molecules. Chemistry of Materials, 2006, 18, 5193-5202.	3.2	59
279	Chemical and Electrical Passivation of Silicon (111) Surfaces through Functionalization with Sterically Hindered Alkyl Groups. Journal of Physical Chemistry B, 2006, 110, 14800-14808.	1.2	114
280	Covalent Attachment of Acetylene and Methylacetylene Functionality to Si(111) Surfaces: Scaffolds for Organic Surface Functionalization while Retaining Siâ^'C Passivation of Si(111) Surface Sites. Journal of the American Chemical Society, 2006, 128, 9990-9991.	6.6	66
281	Chlorinationâ^'Methylation of the Hydrogen-Terminated Silicon(111) Surface Can Induce a Stacking Fault in the Presence of Etch Pits. Journal of the American Chemical Society, 2006, 128, 3850-3851.	6.6	29
282	Comparison of Fisher's linear discriminant to multilayer perceptron networks in the classification of vapors using sensor array data. Sensors and Actuators B: Chemical, 2006, 115, 647-655.	4.0	10
283	Powering the planet: Chemical challenges in solar energy utilization. Proceedings of the National Academy of Sciences of the United States of America, 2006, 103, 15729-15735.	3.3	7,148
284	Chemical Control of Charge Transfer and Recombination at Semiconductor Photoelectrode Surfaces. ChemInform, 2005, 36, no.	0.1	0
285	Comparison of analytical methods and calibration methods for correction of detector response drift in arrays of carbon black-polymer composite vapor detectors. Sensors and Actuators B: Chemical, 2005, 104, 249-268.	4.0	39
286	Chemical and electronic characterization of methyl-terminated Si(111) surfaces by high-resolution synchrotron photoelectron spectroscopy. Physical Review B, 2005, 72, .	1.1	159
287	Chlorination of hydrogen-terminated silicon (111) surfaces. Journal of Vacuum Science and Technology A: Vacuum, Surfaces and Films, 2005, 23, 1100-1106.	0.9	71
288	Low-Temperature STM Images of Methyl-Terminated Si(111) Surfaces. Journal of Physical Chemistry B, 2005, 109, 671-674.	1.2	124

#	Article	IF	CITATIONS
289	High-Resolution X-ray Photoelectron Spectroscopic Studies of Alkylated Silicon(111) Surfaces. Journal of Physical Chemistry B, 2005, 109, 3930-3937.	1.2	101
290	Detection and Classification of Volatile Organic Amines and Carboxylic Acids Using Arrays of Carbon Black-Dendrimer Composite Vapor Detectors. Chemistry of Materials, 2005, 17, 2904-2911.	3.2	120
291	Electrocatalytic hydrogen evolution by cobalt difluoroboryl-diglyoximate complexes. Chemical Communications, 2005, , 4723.	2.2	256
292	Chemical Control of Charge Transfer and Recombination at Semiconductor Photoelectrode Surfaces. Inorganic Chemistry, 2005, 44, 6900-6911.	1.9	149
293	Comparison of the device physics principles of planar and radial p-n junction nanorod solar cells. Journal of Applied Physics, 2005, 97, 114302.	1.1	1,261
294	Detection of Organic Mercaptan Vapors Using Thin Films of Alkylamine-Passivated Gold Nanocrystals. Langmuir, 2004, 20, 299-305.	1.6	33
295	Comparisons between Mammalian and Artificial Olfaction Based on Arrays of Carbon Blackâ^Polymer Composite Vapor Detectors. Accounts of Chemical Research, 2004, 37, 663-672.	7.6	215
296	Anchoring Group and Auxiliary Ligand Effects on the Binding of Ruthenium Complexes to Nanocrystalline TiO2Photoelectrodes. Journal of Physical Chemistry B, 2004, 108, 15640-15651.	1.2	117
297	Current Density versus Potential Characteristics of Dye-Sensitized Nanostructured Semiconductor Photoelectrodes. 1. Analytical Expressions. Journal of Physical Chemistry B, 2004, 108, 5269-5281.	1.2	65
298	Estimation of chemical and physical characteristics of analyte vapors through analysis of the response data of arrays of polymer-carbon black composite vapor detectors. Sensors and Actuators B: Chemical, 2003, 96, 268-282.	4.0	35
299	Mechanism of enhanced sensitivity of linear poly(ethylenimine)-carbon black composite detectors to carboxylic acid vapors. Sensors and Actuators B: Chemical, 2003, 96, 329-342.	4.0	37
300	Comparison of the Electrical Properties and Chemical Stability of Crystalline Silicon(111) Surfaces Alkylated Using Grignard Reagents or Olefins with Lewis Acid Catalysts. Journal of Physical Chemistry B, 2003, 107, 5404-5412.	1.2	199
301	Enhanced Sensitivity to and Classification of Volatile Carboxylic Acids Using Arrays of Linear Poly(ethylenimine)â^'Carbon Black Composite Vapor Detectors. Analytical Chemistry, 2003, 75, 1748-1753.	3.2	44
302	Use of near-surface channel conductance and differential capacitance versus potential measurements to correlate inversion layer formation with low effective surface recombination velocities at n-Si/liquid contacts. Applied Physics Letters, 2002, 80, 4458-4460.	1.5	15
303	Infrared and X-ray Photoelectron Spectroscopic Studies of the Reactions of Hydrogen-Terminated Crystalline Si(111) and Si(100) Surfaces with Br2, I2, and Ferrocenium in Alcohol Solvents. Journal of Physical Chemistry B, 2002, 106, 3639-3656.	1.2	114
304	Properties of Vapor Detector Arrays Formed through Plasticization of Carbon Blackâ^'Organic Polymer Composites. Analytical Chemistry, 2002, 74, 1307-1315.	3.2	66
305	Effects of Interfacial Energetics on the Effective Surface Recombination Velocity of Si/Liquid Contacts. Journal of Physical Chemistry B, 2002, 106, 2950-2961.	1.2	32
306	Exploitation of spatiotemporal information and geometric optimization of signal/noise performance using arrays of carbon black-polymer composite vapor detectors. Sensors and Actuators B: Chemical, 2002, 82, 54-74.	4.0	56

#	Article	IF	CITATIONS
307	Classification performance of carbon black-polymer composite vapor detector arrays as a function of array size and detector composition. Sensors and Actuators B: Chemical, 2002, 87, 130-149.	4.0	47
308	Electron Transfer Dynamics in Nanocrystalline Titanium Dioxide Solar Cells Sensitized with Ruthenium or Osmium Polypyridyl Complexes. Journal of Physical Chemistry B, 2001, 105, 392-403.	1.2	276
309	Investigation of the Size-Scaling Behavior of Spatially Nonuniform Barrier Height Contacts to Semiconductor Surfaces Using Ordered Nanometer-Scale Nickel Arrays on Silicon Electrodes. Journal of Physical Chemistry B, 2001, 105, 12303-12318.	1.2	87
310	Spectroscopic Studies of the Modification of Crystalline Si(111) Surfaces with Covalently-Attached Alkyl Chains Using a Chlorination/Alkylation Method. Journal of Physical Chemistry B, 2001, 105, 10266-10277.	1.2	176
311	Comparison of the Performance of Different Discriminant Algorithms in Analyte Discrimination Tasks Using an Array of Carbon Blackâ^Polymer Composite Vapor Detectors. Analytical Chemistry, 2001, 73, 321-331.	3.2	43
312	Formation of Covalently Attached Polymer Overlayers on Si(111) Surfaces Using Ring-Opening Metathesis Polymerization Methods. Langmuir, 2001, 17, 1321-1323.	1.6	151
313	Array Based Carbon Black-Polymer Composite Vapor Detectors for Detection of DNT in Environments Containing Complex Analyte Mixtures. Materials Research Society Symposia Proceedings, 2001, 700, 411.	0.1	Ο
314	Comparison of odor detection thresholds and odor discriminablities of a conducting polymer composite electronic nose versus mammalian olfaction. Sensors and Actuators B: Chemical, 2001, 72, 41-50.	4.0	68
315	Assessing the ability to predict human percepts of odor quality from the detector responses of a conducting polymer composite-based electronic nose. Sensors and Actuators B: Chemical, 2001, 72, 149-159.	4.0	51
316	Light work with water. Nature, 2001, 414, 589-590.	13.7	243
317	The use of â€~electronic nose' sensor responses to predict the inhibition activity of alcohols on the cytochrome P-450 catalyzed p -hydroxylation of aniline. Bioorganic and Medicinal Chemistry, 2000, 8, 795-805.	1.4	10
318	Role of inversion layer formation in producing low effective surface recombination velocities at Si/liquid contacts. Applied Physics Letters, 2000, 77, 2566-2568.	1.5	29
319	Size-dependent electrical behavior of spatially inhomogeneous barrier height regions on silicon. Applied Physics Letters, 2000, 77, 2698-2700.	1.5	60
320	Preparation of air-stable, low recombination velocity Si(111) surfaces through alkyl termination. Applied Physics Letters, 2000, 77, 1988-1990.	1.5	185
321	Progress in use of carbon-black-polymer composite vapor detector arrays for land mine detection. , 2000, , .		10
322	An Investigation of the Concentration Dependence and Response to Analyte Mixtures of Carbon Black/Insulating Organic Polymer Composite Vapor Detectors. Analytical Chemistry, 2000, 72, 658-668.	3.2	168
323	Cross-Reactive Chemical Sensor Arrays. Chemical Reviews, 2000, 100, 2595-2626.	23.0	1,194
324	Electrochemical and Electrical Behavior of (111)-Oriented Si Surfaces Alkoxylated through Oxidative Activation of Siâ^'H Bonds. Journal of Physical Chemistry B, 2000, 104, 9947-9950.	1.2	50

#	Article	IF	CITATIONS
325	Relationships among Resonant Frequency Changes on a Coated Quartz Crystal Microbalance, Thickness Changes, and Resistance Responses of Polymerâ^'Carbon Black Composite Chemiresistors. Analytical Chemistry, 2000, 72, 2008-2015.	3.2	80
326	Combinatorial Approaches to the Synthesis of Vapor Detector Arrays for Use in an Electronic Nose. ACS Combinatorial Science, 2000, 2, 301-304.	3.3	55
327	High Quantum Yield Sensitization of Nanocrystalline Titanium Dioxide Photoelectrodes withcis-Dicyanobis(4,4â€~-dicarboxy-2,2â€~-bipyridine)osmium(II) or Tris(4,4â€~-dicarboxy-2,2â€~-bipyridine)osmium(II) Complexes. Journal of Physical Chemistry B, 2000, 104, 3488-3491.	1.2	109
328	Preparation and Properties of Vapor Detector Arrays Formed from Poly(3,4-ethylenedioxy)thiopheneâ `Poly(styrene sulfonate)/Insulating Polymer Composites. Analytical Chemistry, 2000, 72, 3181-3190.	3.2	112
329	Sensing and Discrimination of Vapors by an Array of Conducting Carbon Black-Polymer Composites. Digest of Technical Papers SID International Symposium, 1999, 30, 800.	0.1	0
330	Progress in Understanding Electron-Transfer Reactions at Semiconductor/Liquid Interfaces. Journal of Physical Chemistry B, 1998, 102, 4843-4855.	1.2	136
331	Use of Compatible Polymer Blends To Fabricate Arrays of Carbon Blackâ^'Polymer Composite Vapor Detectors. Analytical Chemistry, 1998, 70, 2560-2564.	3.2	79
332	Stabilization of Si Photoanodes in Aqueous Electrolytes through Surface Alkylation. Journal of Physical Chemistry B, 1998, 102, 4058-4060.	1.2	129
333	Quantitative Study of the Resolving Power of Arrays of Carbon Blackâ^'Polymer Composites in Various Vapor-Sensing Tasks. Analytical Chemistry, 1998, 70, 4177-4190.	3.2	159
334	Differential Detection of Enantiomeric Gaseous Analytes Using Carbon Blackâ~'Chiral Polymer Composite, Chemically Sensitive Resistors. Analytical Chemistry, 1998, 70, 1440-1443.	3.2	44
335	Electrochemical Properties of (111)-Oriented n-Si Surfaces Derivatized with Covalently- Attached Alkyl Chains. Journal of Physical Chemistry B, 1998, 102, 1067-1070.	1.2	114
336	Cyclic Voltammetry of Semiconductor Photoelectrodes III:  A Comparison of Experiment and Theory for n-Si and p-Si Electrodes. Journal of Physical Chemistry B, 1998, 102, 4731-4738.	1.2	11
337	Measurement of Interfacial Charge-Transfer Rate Constants at n-Type InP/CH3OH Junctions. Journal of Physical Chemistry B, 1997, 101, 2476-2484.	1.2	45
338	Fermi Golden Rule Approach to Evaluating Outer-Sphere Electron-Transfer Rate Constants at Semiconductor/Liquid Interfaces. Journal of Physical Chemistry B, 1997, 101, 11152-11159.	1.2	117
339	Free-Energy Dependence of Electron-Transfer Rate Constants at Si/Liquid Interfaces. Journal of Physical Chemistry B, 1997, 101, 11136-11151.	1.2	92
340	Array-Based Vapor Sensing Using Chemically Sensitive, Carbon Blackâ^Polymer Resistors. Chemistry of Materials, 1996, 8, 2298-2312.	3.2	608
341	Alkylation of Si Surfaces Using a Two-Step Halogenation/Grignard Route. Journal of the American Chemical Society, 1996, 118, 7225-7226.	6.6	431
342	Rate Constants for Charge Transfer Across Semiconductor-Liquid Interfaces. Science, 1996, 274, 969-972.	6.0	77

#	Article	IF	CITATIONS
343	Limits on the Corrosion Rate of Si Surfaces in Contact with CH3OH-Ferrocene+/0 and CH3OH-1,1'-Dimethylferrocene+/0 Solutions. The Journal of Physical Chemistry, 1995, 99, 5575-5580.	2.9	18
344	Stability of n-Si/CH3OH Contacts as a Function of the Reorganization Energy of the Electron Donor. The Journal of Physical Chemistry, 1995, 99, 8302-8310.	2.9	16
345	The electrical properties of semiconductor/metal, semiconductor/liquid, and semiconductor/conducting polymer contacts. Critical Reviews in Solid State and Materials Sciences, 1993, 18, 327-353.	6.8	39
346	Chemical studies of the passivation of GaAs surface recombination using sulfides and thiols. Journal of Applied Physics, 1991, 70, 7449-7467.	1.1	149
347	Pulse Induced Nanolithography of Graphite in H2O: A Road to Chemical Linkages to the Surface?. AIP Conference Proceedings, 1991, , .	0.3	1
348	Chemical modification of n-gallium arsenide photoanodes with group VIIIB metal ions: stability in contact with 1.0 M potassium hydroxide(aq)-0.10 M dipotassium selenide(aq) solutions and I-V properties in contact with 1.0 M potassium hydroxide(aq)-0.3 M dipotassium telluride(aq) electrolytes. The Journal of Physical Chemistry, 1991, 95, 10133-10142.	2.9	14
349	Short-wavelength spectral response properties of semiconductor/liquid junctions. The Journal of Physical Chemistry, 1990, 94, 6002-6009.	2.9	17
350	Electronic properties of junctions between silicon and organic conducting polymers. Nature, 1990, 346, 155-157.	13.7	85
351	Mechanistic studies of light-induced charge separation at semiconductor/liquid interfaces. Accounts of Chemical Research, 1990, 23, 176-183.	7.6	77
352	Studies of silicon photoelectrochemical cells under high injection conditions. Applied Physics Letters, 1990, 57, 2730-2732.	1.5	12
353	Fabrication of minorityâ€carrierâ€limitednâ€Si/insulator/metal diodes. Applied Physics Letters, 1990, 56, 1919-1921.	1.5	17
354	More efficient solar cells. Nature, 1990, 345, 293-294.	13.7	17
355	Efficient photovoltaic devices for InP semiconductor/liqud junctions. Nature, 1989, 340, 621-623.	13.7	19
356	"Ideal" behavior of the open circuit voltage of semiconductor/liquid junctions. The Journal of Physical Chemistry, 1989, 93, 3735-3740.	2.9	95
357	Studies of the gallium arsenide/potassium hydroxide-selenium ion (Se22-)/selenide semiconductor/liquid junction. The Journal of Physical Chemistry, 1989, 93, 3260-3269.	2.9	33
358	Preparation of STM tips for <i>inâ€situ</i> characterization of electrode surfaces. Journal of Microscopy, 1988, 152, 651-661.	0.8	51
359	Applications of Scanning Tunneling Microscopy to Electrochemistry. ACS Symposium Series, 1988, , 174-201.	0.5	5
360	Chemical modification of n-GaAs electrodes with Os3+ gives a 15% efficient solar cell. Nature, 1987, 326, 861-863.	13.7	59

#	Article	IF	CITATIONS
361	630â€mV open circuit voltage, 12% efficientn‧i liquid junction. Applied Physics Letters, 1984, 45, 423-425.	1.5	60
362	7.2% efficient polycrystalline silicon photoelectrode. Applied Physics Letters, 1984, 44, 539-541.	1.5	11
363	A 14% efficient nonaqueous semiconductor/liquid junction solar cell. Applied Physics Letters, 1984, 45, 1095-1097.	1.5	87
364	Systematic studies of the semiconductor/liquid junction: n-gallium arsenide phosphide anodes in aqueous selenide (Se2-/Se22-) solutions. The Journal of Physical Chemistry, 1984, 88, 1310-1317.	2.9	17
365	Evidence against surface state limitations on efficiency of p-Si/CH3CN junctions. Nature, 1984, 307, 533-534.	13.7	28
366	A Quantitative Investigation of the Open ircuit Photovoltage at the Semiconductor/Liquid Interface. Journal of the Electrochemical Society, 1984, 131, 2496-2503.	1.3	112
367	Chemistry: A novel solar cell. Nature, 1983, 305, 671-671.	13.7	6
368	nâ€ŧype GaAs photoanodes in acetonitrile: Design of a 10.0% efficient photoelectrode. Applied Physics Letters, 1983, 43, 115-117.	1.5	32
369	Improvement of photoelectrochemical hydrogen generation by surface modification of p-type silicon semiconductor photocathodes. Journal of the American Chemical Society, 1982, 104, 467-482.	6.6	330
370	Design of a 13% efficient n-GaAs1â^'xPx semiconductor–liquid junction solar cell. Nature, 1982, 300, 733-735.	13.7	50
371	Heterogeneous electron transfer at designed semiconductor/liquid interfaces. Rate of reduction of surface-confined ferricenium centers by solution reagents. The Journal of Physical Chemistry, 1980, 84, 2033-2043.	2.9	34
372	Photoelectrochemical reduction of N,N'-dimethyl-4,4'-bipyridinium in aqueous media at p-type silicon: sustained photogeneration of a species capable of evolving hydrogen. Journal of the American Chemical Society, 1979, 101, 7721-7723.	6.6	66
373	Chemically derivatized n-type silicon photoelectrodes. Stabilization to surface corrosion in aqueous electrolyte solutions and mediation of oxidation reactions by surface-attached electroactive ferrocene reagents. Journal of the American Chemical Society, 1979, 101, 1378-1385.	6.6	141
374	CHAPTER 3. Structured Materials for Photoelectrochemical Water Splitting. RSC Energy and Environment Series, 0, , 52-82.	0.2	9
375	Selective-Area, Water-Free Atomic Layer Deposition of Metal Oxides on Graphene Defects. ACS Materials Au, 0, , .	2.6	1
376	Numerical Simulation and Modeling of Hydrogen Gas Evolution on Planar and Microwire Array Electrodes. Journal of the Electrochemical Society, 0, , .	1.3	0